Advanced Steel Construction – Vol. 19 No. 3 (2023) 209–222
DOI:10.18057/IJASC.2023.19.3.3

THE BENDING BEHAVIOR AND FREE VIBRATION OF THE CONCRETE-STEEL COMPOSITE FLOORS

Sadiq Ahmad Afzali [1], Çağlar Özer [2], Barış Bayrak [1], Ahmad Jamshid Sadid [1], Oğuzhan Çelebi [1] and Abdulkadir Cüneyt Aydın [1, *]

[1] *Ataturk University, Engineering Faculty, Department of Civil Engineering, 25030, Erzurum, Turkey*

[2] *Ataturk University, Earthquake Research Center, Erzurum, Turkey*

** (Corresponding author: E-mail: acaydin@atauni.edu.tr)*

A B S T R A C T

The paper aims to investigate the bending behavior and free vibration of the concrete-steel composite floors, including high temperatures. The inspected properties are analyzed for the maximum displacement, load capacity, energy absorption capacity, and acceleration by using bending tests for varying stud density and elevated temperatures. Withal, bolts are used as studs throughout this study. The result of bending tests implies that, decreasing the spacing of the studs and the addition of mesh reinforcement and steel fiber will increase the energy absorption and maximum load capacity of the steel composite floors. Besides, the increasing the stud density reduces the vibration response of the composite floors, and the mesh reinforcement eliminates the efficiency of the steel fiber on the vibration response of the steel composite floors. Meanwhile, increasing the steel-fiber content causes the reduction in the vibration response of the slabs exposed to high temperatures.

A R T I C L E H I S T O R Y

Received: 12 September 2022
Revised: 5 March 2023
Accepted: 3 April 2023

K E Y W O R D S

Composite floor;
Cold-formed steel;
Steel fiber;
Vibration;
Bending;
High temperature

1. Introduction

Steel composite floors are considered as an alternative to the commonly used conventional reinforced concrete floors. Steel composite floors are generally preferred in recreational, commercial, industrial, and residential buildings due to their fast construction process and safe and economical construction methods. Structurally, composite flooring meets all needs in terms of providing the sufficient strength and durability stipulated by the standards. Composite floors consist of steel sheets, plain or reinforced concrete, and connectors. The strength and ductility of the steel-concrete composite floors depend on various factors such as the geometry of the profiled sheeting, layout and position of the connectors used to ensure composite action between the steel sheeting, the reinforced concrete, and the thickness of the profiled sheeting [1-4]. In addition, steel composite floors, which can also be used as reinforcement elements in structural systems, can also resist bending (positive and negative moment) moments in both directions [5]. Steel sheet, which is one of the components of steel composite flooring, can be used not only as a mold but also in cases where tensile stresses are intense [6]. In addition to materials such as steel sheet, conventional concrete and studs that make up the composite flooring, it is also aimed to reduce the stresses and vibrations caused by possible bending of the flooring by using steel fiber in the flooring. Steel fibers increase the shear and bending strength after cracks occur, allowing effective stress to spread uniformly between these cracks [7]. Studs are widely used in structures to meet the shear forces between composite materials, especially at the floors. The dynamic and/or static loads result in the shear force and bending moment at the floors. In addition, it can be exposed to environmental vibration, earthquake, wind, explosions and vibration, caused by machines on the floor. Such vibrations can cause undesirable deflections and horizontal displacements in the structure. Furthermore, these vibrations negatively affect human comfort and can also damage some important equipment in the building [8]. Therefore, floor vibrations must be considered in the structural design or evaluation [9].

In recent years, the composite floors have been in great demand, due to their light weight, affordability, and ability to respond to natural disasters, such as earthquakes. However, the free or forced vibration behavior of composite floors is a very familiar phenomenon. The most common practice to improve the quality of composite floors is to identify and suppress the unwanted vibrations, as vibration can cause discomfort, serviceability problems, and direct failure of the structure. Several studies on the determination of the dynamic characteristics of the structural floor systems have been performed with an emphasis on the natural frequencies of the floor systems. Ferreira and Fasshauer [10] performed a study on the free vibration of symmetric composite plates based on an innovative numerical scheme. The results of different thickness-to-length ratios were determined and discussed in the study. Ju et al. [11] performed experimental tests to measure the natural frequencies and damping ratios of a new composite floor system. The composite floor systems consisting of steel beams and concrete slabs were examined, and the results were compared with the design codes to evaluate the serviceability of the system in three construction stages (steel erection stage, concrete casting stage, and finishing stage). Gandomkar et al. [12] experimentally and numerically investigated the effect of parameters such as screw spacing, steel profiled sheet thickness, and dry board thickness on the natural frequencies of a composite floor system by the name of profiled steel sheet dry board (PSSDB). Furthermore, Gandomkar et al. [13] measured the natural frequencies of profiled steel sheet dry board floors infilled with concrete (PSSDBS). Hector and Fernando [14] conducted an experimental study to determine the shear behavior of composite slabs according to Eurocode 4. In order to examine the shear behavior, cracks were observed with cyclic loading in composite slabs designed differently from each other. Hick et al. [15] investigated the contribution of the use of studs to the shear resistance of composite slabs formed with steel profiles with a span of 11.4 m. The results showed that the effect of stud should be considered in three-point bending tests. Costa-Neves et al. [16] specified the modes of vibration and natural frequencies of the composite steel deck floor system in a multi-story, multi-bay building. They used the system's natural frequencies to determine its comfortableness. Jarnerö et al. [17] experimentally investigated the natural frequencies, mode shapes, and damping ratio of a prefabricated timber floor system in unusual boundary conditions and different construction stages. The main concerns about composite slabs are mostly focused on the shear bond, shear resistance, flexural strength, and slip behavior, including cast screws [11, 12, 16, 17]. Holomek et al. [18] conducted a series of experiments to investigate the effects of cast screws diameters and structural element layouts on the bending capacity of composite slabs. The results showed that small-diameter screws were effective at small shear forces, while large ones were efficient at-large shear forces.

This study aims to investigate the effect of the shear stud density on the vibration response and bending behavior of the steel composite floors, including the post-fire response. Meanwhile, the spacing of the studs, steel fiber content, and the mesh reinforcement were considered as the parameters of the investigation. The high-temperature, steel fibers, stud density, and reinforcement effect with free vibration for bending are inspected, also.

2. Experimental work

2.1. Material properties and specimens

In this investigation, 18 steel-concrete composite floor models were prepared using three types of concrete mixes (conventional concrete and two types of steel fiber reinforced concrete). The concrete mixes was produced according to the Turkish Standard TS802 [19], using CEM II/A-M(P-LL) 42.5 R cement and 16 mm maximum size aggregate. The hooked steel fiber (Fig. 1a) with the geometric dimension of length (L) = 35 mm, diameter (d) = 0.55 mm, and the aspect ratio (L/d) = 65 with a nominal tensile strength of 1.345 MPa and young's modulus of 2×105 MPa was selected according to TS/EN-14889-1 [20]. The amount of steel fiber for the steel fiber reinforced concrete (SFRC) was chosen as 30 kg/m^3 and 60 kg/m^3 of the total volume of the model. The no-fiber type reference samples presented a compressive strength as 50 MPa, where the similar strength values were 48 and 43 MPa for the samples with 30 kg/m^3 and 60 kg/m^3 steel fibers, respectively. The galvanized cold-formed steel sheet was used with the dimensions of 860x27x0.5 mm, for the floor decking of the models. M6*80 mm pan-headed bolts with EPDM bonded sealing washers were used for strengthening the shear bond between concrete and the steel sheet (Fig. 1b). To observe the stud density effect, the spans for bolt-type studs are designed for 22 and 55 cm. Furthermore, for the models, the Q188/188 mesh reinforcements (Fig. 1c) were used according to TS4559 [21].

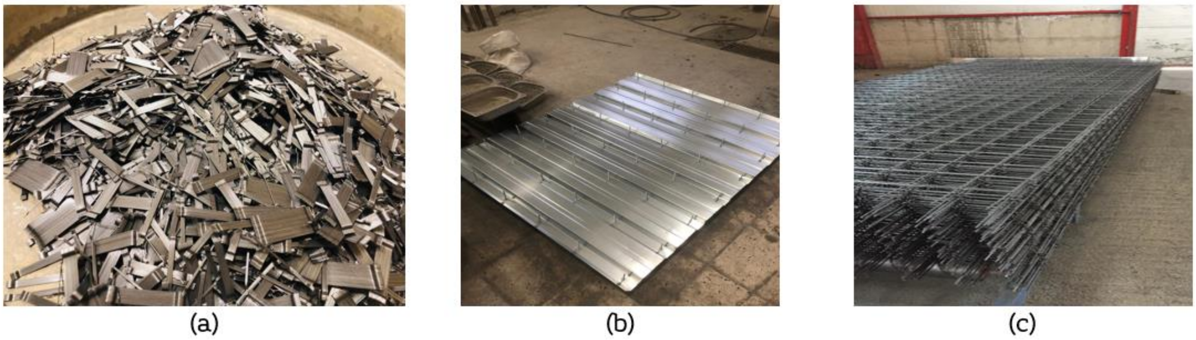

Fig. 1 Composite floor components used in the study

In this investigation, there are two groups of models. The first group of models includes 12 steel-composite floors fabricated with an aspect ratio of 0.8 (1500 mm x 1200 mm), and the second group includes 6 with an aspect ratio of 0.92 (760 mm x 700 mm). The second group of the models is designed according to high-temperature furnace for three hours of 600 ^{0}C (6 hours from room temperature to 600 ^{0}C, 3 hours at 600 ^{0}C, and 8 hours from 600 ^{0}C to room temperature). The thickness of all the models is considered as 110 mm. The type of concrete, the spacing of the bolts, and the reinforcement are the main variables of the models. The specifications and dimensions of the models are presented in Table 1 and Fig. 2.

Table 1
Properties of composite floor models

Model Code	Type of Concrete (Compressive Strength)	Steel Fiber Ratio in Concrete (Kg/m^3)	Bolts Spacing (mm)	Mesh Reinforcement
		Group 1 of Models (1500 mm x 1200 mm)		
CC22M	Conventional Concrete	0	220	With Mesh
CC55M		0	550	With Mesh
CC22		0	220	Without Mesh
CC55		0	550	Without Mesh
30SFRC22M	30 kg/m^3 SFRC	30	220	With Mesh
30SFRC55M		30	550	With Mesh
30SFRC22		30	220	Without Mesh
30SFRC55		30	550	Without Mesh
60SFRC22M	60 kg/m^3 SFRC	60	220	With Mesh
60SFRC55M		60	550	With Mesh
60SFRC22		60	220	Without Mesh
60SFRC55		60	550	Without Mesh
		Group 2 of Models (760 mm x 700 mm)		
FCC22M	Conventional Concrete	0	220	With Mesh
FCC22		0	220	Without Mesh
F30SFRC22M	30 kg/m^3 SFRC	30	220	With Mesh
F30SFRC22		30	220	Without Mesh
F60SFRC22M	60 kg/m^3 SFRC	60	220	With Mesh
F60SFRC22		60	220	Without Mesh

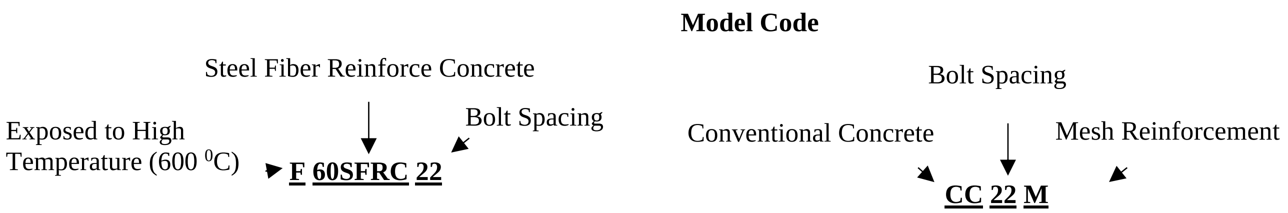

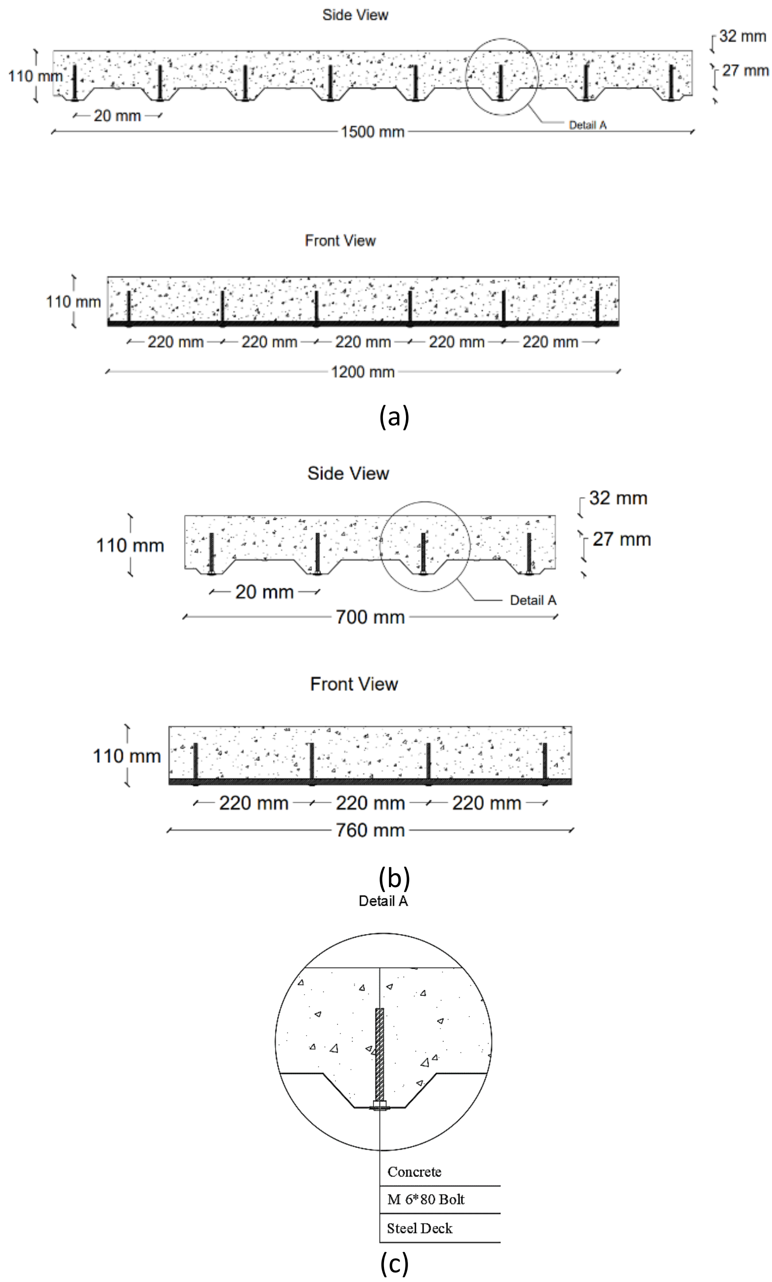

Fig. 2 Geometric dimensions of tested models (a) Group 1 (b) Group 2 (c) Composite floor bolt detail

Table 2
Concrete mixing ratios

Concrete type	Cement kg/m^3	Sand (0-4 mm) kg/m^3	Aggregate (4-16 mm) kg/m^3	Water kg/m^3	Steel fiber kg/m^3
Conventional concrete	370	448.54	1345	206.614	0
30SFRC	365.317	442.87	1328.47	204	30
60SFRC	360.64	437.2	1311.45	201.4	60

2.2. Test setup and procedure

2.2.1. Concrete experiments

As the main component of the composite floors, the concrete, with or without fibers, was tested for the mechanical properties. The concrete mixture calculation was made according to TS 802 [19] (Table 2), and a total of 18 concrete samples were prepared to be placed in 15x15x15 cm cube, 10x10x40 prism and 10x20 cylinder molds (Fig. 3a). The obtained concrete samples were kept in a curing environment at 22 °C for 28 days and subjected to compression and bending tests. The compression and bending tests were realized according to TS EN 12390-3 [22] and TS EN 12390-5 [23], respectively. Then, relevant tests were also repeated for the samples with the 30 or 60 kg/m^3 steel fibers. The placement of the studs to the steel sheet before concrete pouring is shown in Fig. 3b and after the concrete is poured, the composite floor is presented in Fig. 3c. The 28 days- compression and flexural test results of three mixtures are given in Table 3. Furthermore, the stress-strain curves of samples observed from the compressive strength tests are also shown in Fig. 4. The mean value of three samples was used while drawing the stress-strain curve.

Table 3
Hardened concrete test results

	Compressive strength			Flexural strength		
Concrete type/Sample	Conventional concrete	30SFRC	60SFRC	Conventional concrete	30SFRC	60SFRC
Sample 1	50.42	49.81	42.35	3.80	4.44	4.32
Sample 2	46.95	47.15	41.67	4.15	4.33	4.64
Sample 3	50.08	46.71	44.40	4.09	4.20	4.84
Average	49.15	47.89	42.81	4.01	4.32	4.60

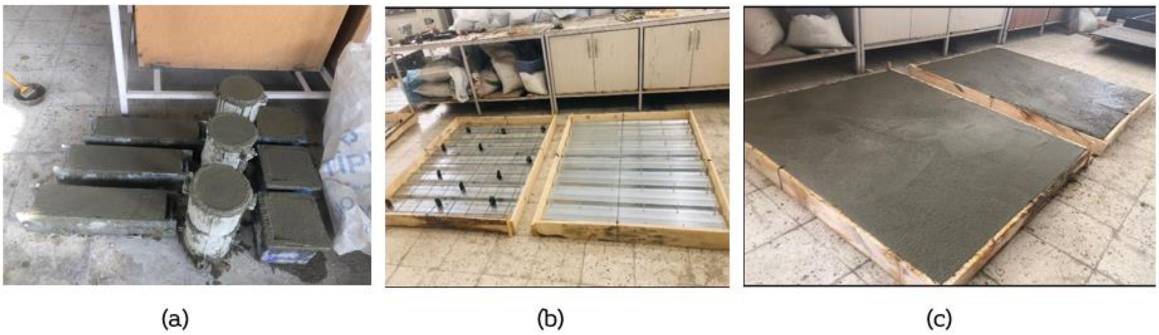

Fig. 3 Concrete mixture experiments: a) Concrete poured into cube, cylinder and prism molds b) Placement of the studs to the sheet steel without concrete c) Model composite floor

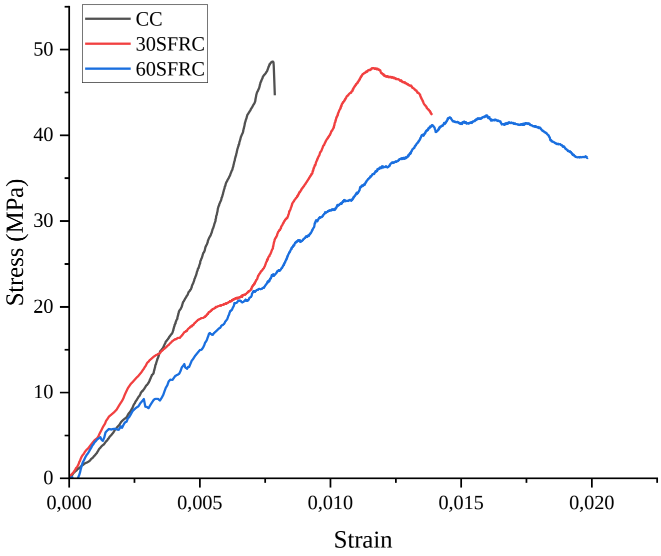

Fig. 4 Stress-strain curve of samples

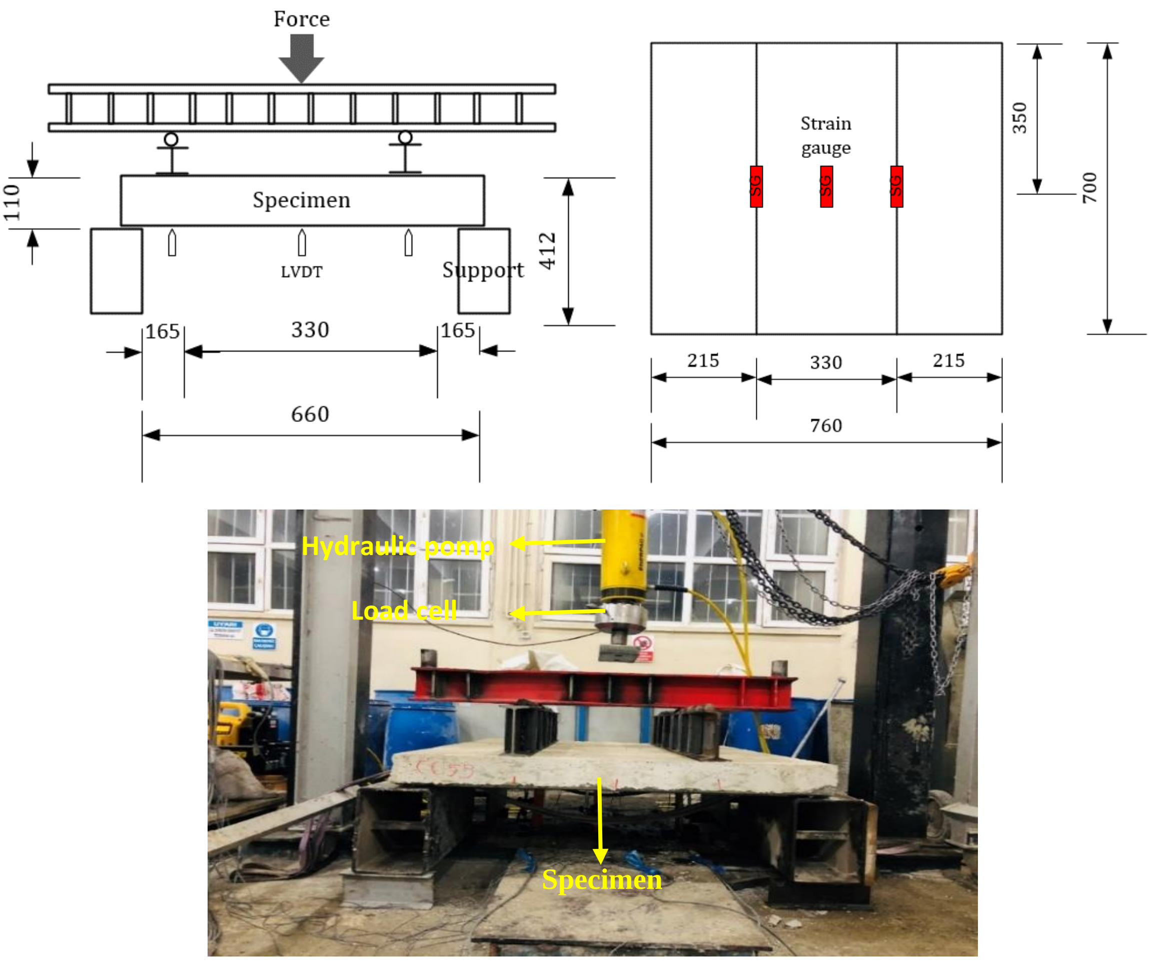

Fig. 5 The bending test setup, the positions of LVDTs, and strain gages of the models (all units are mm)

2.2.2. Bending test setup

The bending tests were to measure the bending capacities and corresponding deformations of composite floors formed with different fiber ratios and mesh reinforcements. The effects of steel fibers, stud placement, high temperature, and mesh reinforcements on the bending capacities, and the deformation abilities of the slabs were determined by bending tests. The orientation and the drawing of the experimental setup can be seen at Fig. 5. Thus, the hydraulic pump with a load capacity of 1000 KN is in a position to apply a uniform load to the entire floor resting on two horizontally placed supports (Fig. 4a). The bending tests of the models were prepared according to the Eurocode-4 [24]. To measure the vertical displacement of the models, the LVDTs (Linear Variable Displacement Transducers) were placed vertically in three positions under the floor systems. Besides, the strain gauges were attached to each model to measure the deformations of the steel sheet. Fig. 5 shows the bending test setup, the positions of LVDTs, and strain gages of the models.

2.2.3. Vibration test setup

The accelerometer tests were applied to measure possible vibrations that may occur on the samples. The effect of steel fibers, placement of studs, high-temperature, and mesh reinforcements on vibrations have been investigated, by using accelerometer data for the region where the sample would likely deflect the most (Fig. 6a). The vibration test experimentation is shown in Fig. 6b. Within the light of the literature, the digital accelerometer (CMG-5TD) was placed to area, where the moment is maximum [25]. The sensor was positioned and fixed using the provided screws to the surface of the model and connected to the PC.

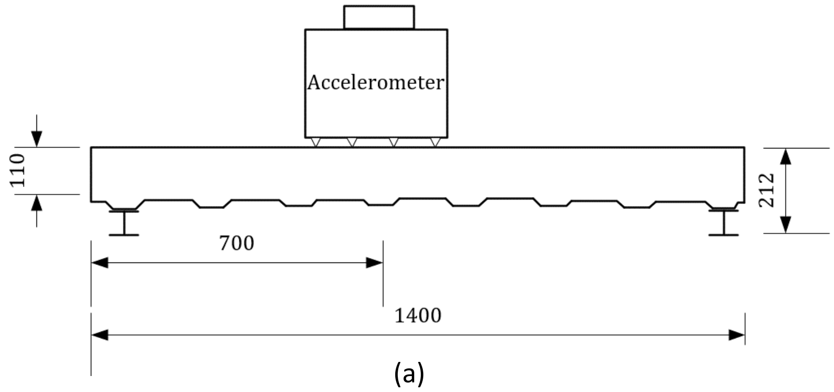

(a)

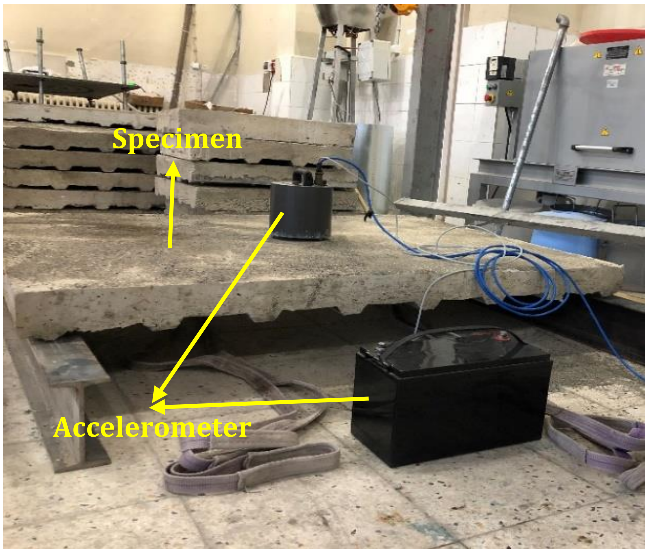

(b)

Fig. 6 The vibration test setup: a) Placement on slab of accelerometer b) Application of vibration test

2.2.4. High temperature related experiments

In this part, the models were kept at 600 °C for 3 hours to observe the changes in bending capacities and vibration parameters, when the samples with different steel fiber contents and exposed to high temperatures. For this experiment, a digitally controlled high-temperature furnace with a heating capacity of 1200 °C was used. After the models were kept at 600 °C for 3 hours. Then, they were removed from the high-temperature furnace, after getting waited to cool down to room temperature (8 hours from 600 ^{0}C to room temperature), for the vibration and bending tests. Fig. 7a and Fig. 7b shows the high-temperature furnace, and the models placed.

(a) (b)

Fig. 7 High-temperature experiments: a) high-temperature furnace b) models in the furnace

3. Results and discussions

3.1. Bending test

3.1.1. The effect of bolt spacing on the behavior of the composite floors

Fig. 8 is obtained according to the bending test results. As shown, the decreasing stud (bolt) spacing increased the bending and energy absorption capabilities, as the fiber ratio increase.

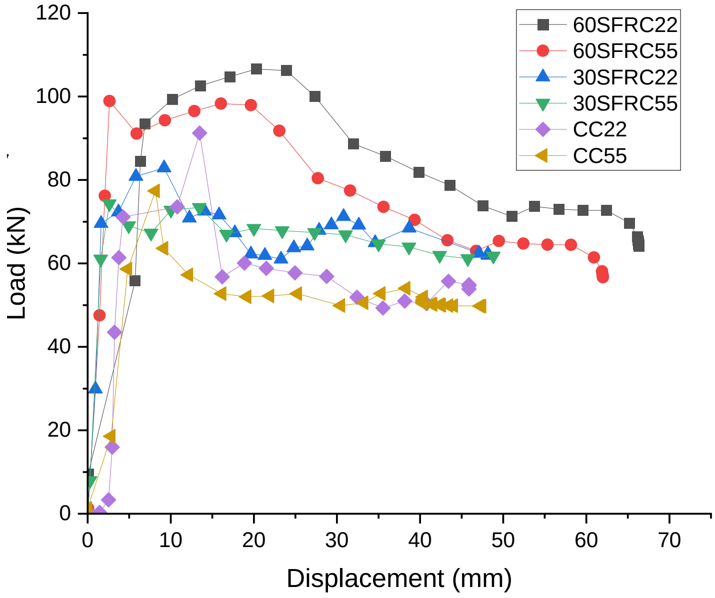

Fig. 8 Load-displacement graph for CC55, CC22, 30SFRC55, 30SFRC22, 60SFRC55 and 60SFRC22

Table 4
The effect of bolts spacing on the behavior of composite floors

Model Code	Energy Absorption (kN*mm)	Difference in Energy Absorption (%)	Maximum Load (kN)	Maximum Displacement at the center point (mm)
		CC		
CC55	2415.35	+7.46	77	8
CC22	2595.56		90	14
		30SFRC		
30SFRC55	3204	+1.62	74	2.6
30SFRC22	3256		82	9
		60SFRC		
60SFRC55	4821.51	+12.97	99	16
60SFRC22	5447.15		106	20

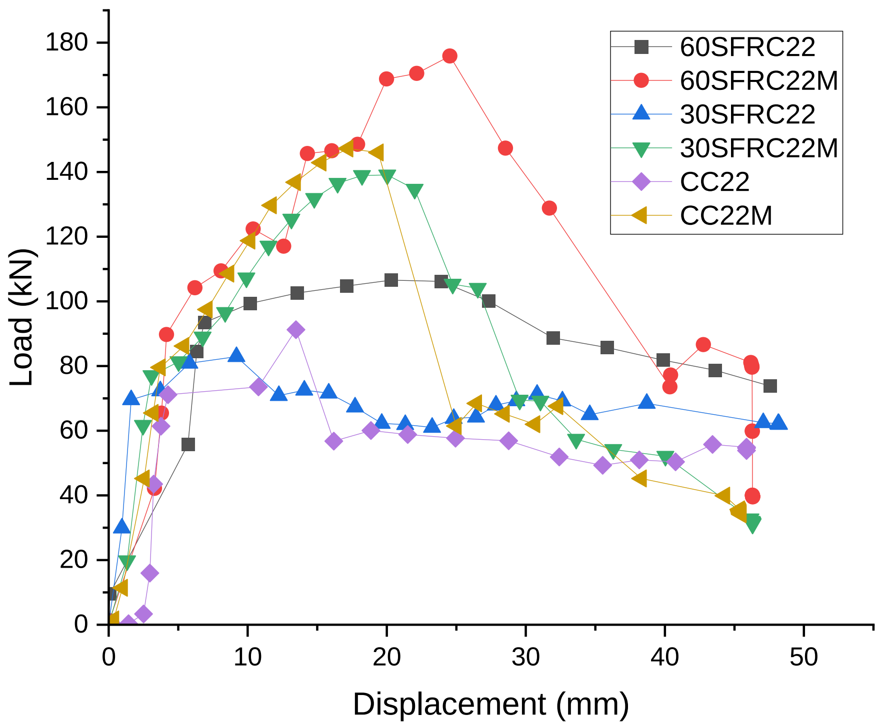

Fig. 9 Load-displacement graph for CC22 and CC22M, 30SFRC22, 30SFRC22M, 60SFRC22 and 60SFRC22M

3.1.2. The effect of mesh reinforcement on the behavior of composite floors

According to the results of the bending tests, it has been determined that the bolt spacing is at 22 cm, which has the highest bending, displacement and energy absorption capacity. Therefore, to determine the effectiveness of the mesh reinforcement, the models with a bolt spacing of 22 cm were taken as a reference in the test results. As seen in Table 5 and Fig. 9, the energy adsorption capability was increased by 43.47% for the conventional concrete models. Withal, these increments were 21.16%, and 31.34%, for the steel fiber reinforced ones with 30 kg/m^3 and 60 kg/m^3, respectively. The displacements of the CC22 and CC22M models were increased linearly in the loading interval of 0-90 kN and 0-150 kN. The displacements corresponding to the maximum load for CC22 and CC22M models were determined as 14 mm and 17 mm, respectively. Similarly, the displacement at the center points of 30SFRC22 and 30SFRC22M models increased linearly in the loading interval of 0-82 kN and 0-80 kN. The displacements corresponding to the maximum load for the 30SFRC22 and 30SFRC22M models were determined as 9 mm and 18 mm. Furthermore, the displacements of 60SFRC22 and 60SFRC22M were increased linearly in the loading interval of 0-106 kN and 0-176 kN, and the displacement corresponding to the maximum load for 60SFRC22 and 60SFRC22M were 20 mm and 24 mm, respectively.

The maximum load capacities were increased by 62.85%, 64.66%, and 65.56% for the CC, 30SFRC, and 60SFRC models. Furthermore, the displacements at the maximum load were increased by 32.96%, 216.58%, and 2.63% for the CC, 30SFRC, and 60SFRC samples. The bending tests have shown that, the use of mesh reinforcements in combination with steel fibers in composite flooring gives higher bending and displacement capability, then the ones with conventional concrete. Although, the increase in the amount of steel fiber in composite floors with mesh reinforcement did not change the bending capacity much, it was determined that, the displacement capacity decreased significantly. In addition, the after-test photos of the samples (failure mode) are shown in Fig. 10.

Table 5

The effect of mesh reinforcement on the behavior of composite floors

Model Code	Energy Absorption (kN*mm)	The difference in Energy Absorption (%)	Maximum Load (kN)	Maximum Displacement at the center point (mm)
		CC		
CC22	2595.56	+43.47	90	14
CC22M	3723.86		150	17
		30SFRC		
30SFRC22	3256	+21.16	82	9
30SFRC22M	3945.06		140	18
		60SFRC		
60SFRC22	4089.97	+31.34	106	20
60SFRC22M	5371.65		176	24

Fig. 10 Failure mode of tested samples a) CC22 b) CC22M c) 30SFRC55 d) 30SFRC55M e) 60SFRC55

3.1.3. The effect of steel fiber reinforcement on the behavior of composite floors

As seen in Table 6, when the steel-fiber is added to the mixture, the energy absorption capacity is increased by 25.45 % for the models with 30 kg/m^3 steel-fiber, where this increment was 57.58 % for the ones with 60 kg/m^3 for the steel-fibers. The maximum load capacity of the composite floors were decreased by 8.89% and increased by 17.78% for the 30SFRC and 60SFRC models. The displacements at the maximum load were decreased by 35.71% and increased by 42.86% for the 30SFRC and 60SFRC models. As expected, increasing the steel fiber content to 30 kg/m^3 resulted less load carrying capability, but greater deformation capability, when compared to conventional concrete models. Which means, more permanent deformation and more energy absorption capability without sudden collapse.

Table 6
The effect of steel fiber reinforcement on the behavior of composite floors

Model Code	Energy Absorption (KN*mm)	The difference in Energy Absorption (%)	Maximum Load (KN)	Maximum Displacement at the center point (mm)
CC22	2595.56	-	90	14
30SFRCC22	3256.00	+25.45	82	9
60SFRCC22	4089.97	+57.58	106	20

Fig. 11 shows the load displacement at the center point of the models. The displacements of the CC22, 30SFRC22, and 60SFRC22 models were increased linearly in the 0-90 kN, 0-82 kN, and 0-06 kN loading ranges. If it is desired to create composite flooring with only steel fiber reinforcement, without the use of mesh reinforcement, it is foreseen that the amount of fiber should be adjusted optimally. Because, it is obvious that the energy absorption capacity, bending strength and permanent deformation of the model with 60 kg/m^3 steel fiber content was higher than that of the one with 30 kg/m^3 steel fiber content. In addition, the permanent deformation without sudden load changes of the model containing 60 kg/m^3 steel fiber and loss of permanent deformation ability, as sudden load loss for the one with 30 kg/m^3 steel fiber indicates the optimum amount of the steel fiber.

Fig. 12 has been drawn to compare the energy absorption, load carrying, and permanent strain capacities of the Group 1 samples concerning each other. As shown in Fig. 12a, the flooring with the highest energy absorption capacity was the model with 60 kg/m^3 steel fiber content, 22 cm bolt (stud) spacing, and no mesh reinforcement. In this case, it is understood that the steel fiber and the bolt spacing contribute significantly to the ductility of the flooring. In Fig. 12b, it is seen that the composite flooring with 60 kg/m^3 steel fiber content, mesh reinforcement and 22 cm bolt spacing has the highest load-carrying capacity. It has been determined that the increase in the amount of steel fiber, the reduction of the bolt spacing and the use of mesh reinforcement increase the load capacity of the flooring. In Fig. 12c, it is observed that the composite flooring with 60 kg/m^3 fiber content, no mesh reinforcement and 22 cm bolt spacing has the highest displacement capacity. It has also been determined that the displacements of the model, in which the steel fiber and mesh reinforcement are used together, are not much different from the displacements of the only conventional concrete-containing model.

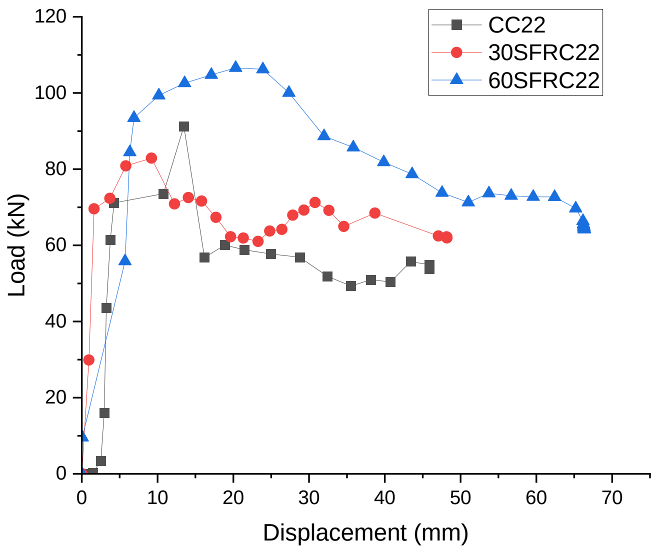

Fig. 11 Load-displacement graph for CC22, 30SFRC22 and 60SFRC22

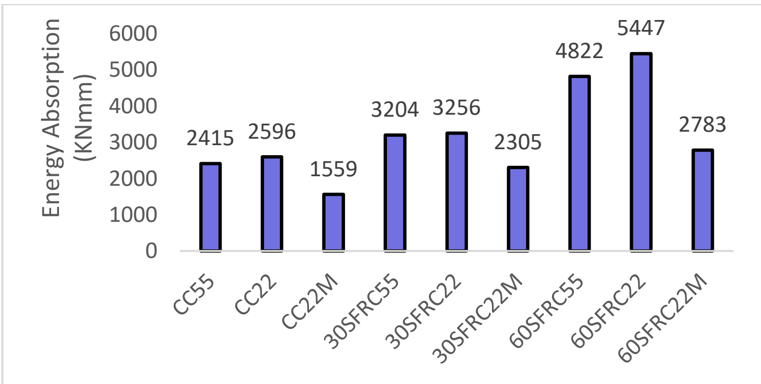

(a)

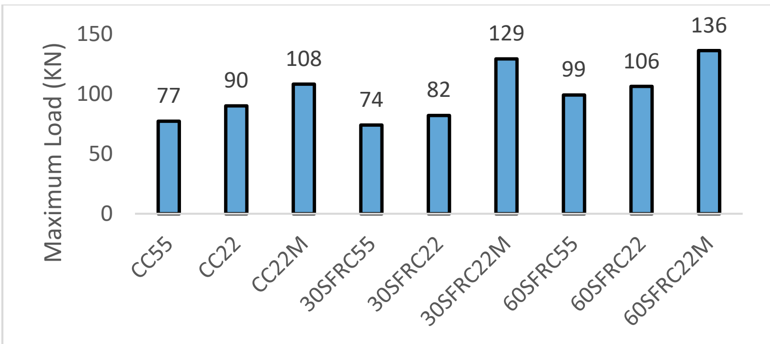

(b)

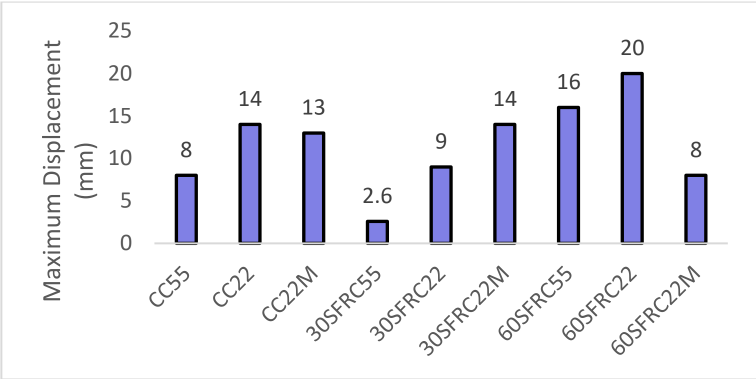

(c)

Fig. 12. Bending test results of the 1st group samples: a) energy absorption b) Capacity of load c) Capacity of displacement

3.1.4. The effect of mesh reinforcement and steel fiber reinforcement on the behavior of models exposed to high temperatures

The load-displacement graph of the models exposed to high-temperature is shown in Fig. 13. The displacements of the FCC22, FCC22M, F30SFRC22, F30SFRC22M, and F60SFRC22 models increased linearly with increasing the load up to 61 kN, 108 kN, 88 kN, 129 kN, and 105.88 kN respectively. The displacements corresponding to the maximum load of these models were determined as 20 mm, 13 mm, 14 mm, 14 mm, 19.8 mm and 8 mm.

As shown in Table 7, when the mesh reinforcement is added to the models, the effect of elevated temperature to energy absorption capacity is increased by 52.26 % in conventional concrete, by 39.07 % for the models with 30 kg/m^3 steel fibers, and by 22.92 % for the ones with 60 kg/m^3 steel fibers. After the high-temperature process, the observed maximum load was increased by for the CC model. However, the same observation for the 30SFRC, and 60SFRC models were indicated an increase by 46.59% and 28.45%, respectively. When the steel fiber is added to the concrete mixture, the energy absorption capacity is increased by 61.86% and 121.09% in 30 kg/m^3 reinforced steel fiber concrete, and 60 kg/m^3 reinforced steel fiber concrete. Besides, the maximum load capacities of the models were increased by 44.26% and 73.57% for the 30SFRC and 60 SFRC ones. Furthermore, the displacements corresponding to the maximum load were decreased by 30% and 1% for the 30SFRC and 60SFRC models, respectively.

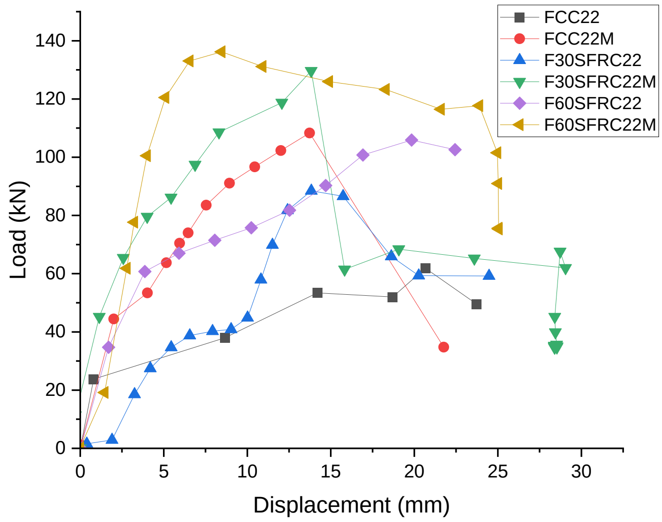

Fig. 13 Load-displacement graph for FCC22, FCC22M, F30SFRC22, F30SFRC22M, F60SFRC22, and F60SFRC22M)

Table 7

The effect of mesh reinforcement and steel fiber reinforcement on the behavior of composite floors exposed to high temperatures

Model Code	Energy Absorption Area (KN*mm)	The difference in Energy Absorption (%)	Maximum Load (KN)	Maximum Displacement at the center (mm)
		CC		
FCC22	1024	+52.26	61	20
FCC22M	1559.11		108	13
		30SFRC		
F30SFRC22	1657.46	+39.07	88	14
F30SFRC22M	2305.09		129	14
		60SFRC		
F60SFRCC22	2264	+22.92	105.88	19.8
F60SFRC22M	2783		136	8

3.2. Vibration response

In this study, the vertical vibrations were obtained by placing CMG-5TD accelerometers on the model slabs made of 30 kg/m^3 and 60 kg/m^3 steel fiber with conventional concrete with varying stud spacings. The vibrations were measured in 1st group models (1500 x 1200 mm) and 2nd group models (760x700 mm) after the high-temperature process. The vibration records, applied in 0.01 s time steps in the time history, were filtered in the frequency range of 0.5-25 Hz to obtain internal vibration data from the sample. The natural frequencies of the models were determined by using Fourier transforms (FFT) [26]. The frequency environment of the models with varying stud spacings and mesh reinforcements, for the conventional concrete were presented in Fig. 14. The 1st mode natural frequencies of the CC22, CC22M, CC55M and CC55 models were determined as 10.53, 20.44, 11.82 and 13.99 Hz, respectively. It was determined that, reducing the screw (stud) spacing from 55 cm to 22 cm, the natural frequency was reduced by 10.92% for the no-mesh model, and by 31.67% for the one with mesh. Withal, the use of mesh reinforcement was shown that, the oscillations were reduced by approximately 50% for the models with 22 cm screw spacing, and 14% for the ones with 55 cm screw spacing. The 2nd mode frequencies of the CC22, CC22M, CC55 and CC55M models were obtained as 12.95, 21.02, 17.18, and 20.8 Hz, respectively. The 3rd mode frequencies of the models were determined as 23.7 Hz. The CC55 model had the highest amplitude between the ones at the same frequency. It was noted that in this group of models, the arrangement of the mesh reinforcement and the 22 cm screw spacing present the most optimum results.

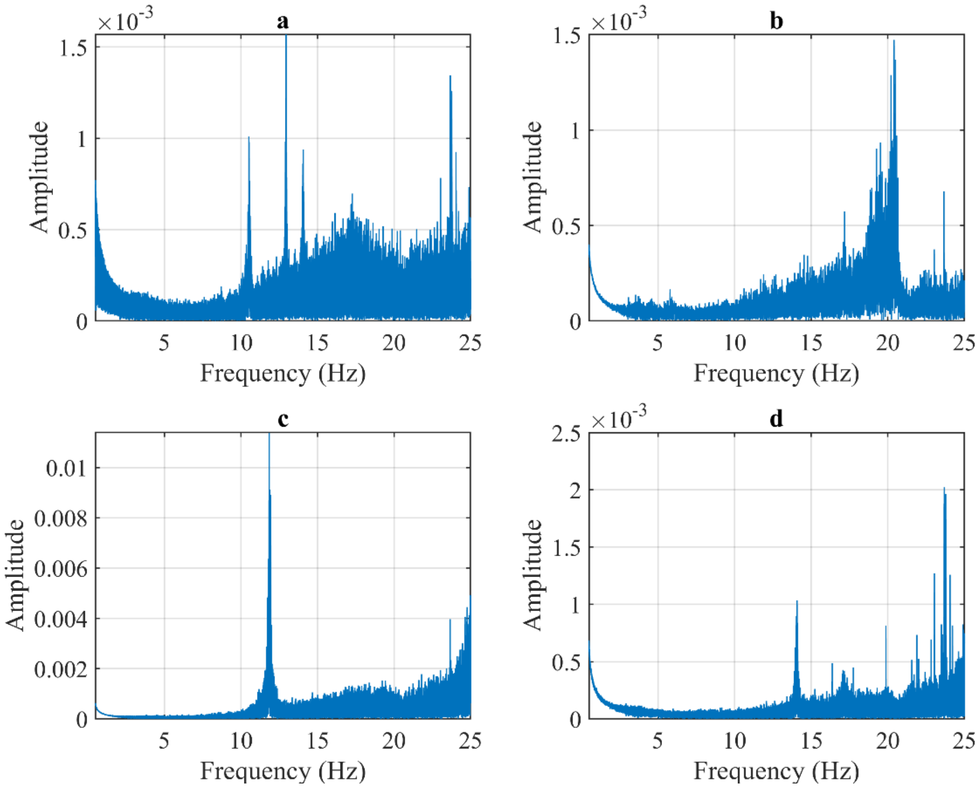

Fig. 14 Frequency of the models with conventional concrete and mesh a) CC22 b) CC22M c) CC55 d) CC55M

The frequency calculations, obtained for the models with 30 kg/m^3 fibers are presented in Fig. 15. It has been determined that, the use of 30 kg/m^3 steel fiber with 22 cm screw spacing was increased the natural frequency of the flooring from 10.53 Hz to 12.67 Hz. The natural frequency, for the model with mesh reinforcement and same screw spacing, was decreased from 20.44 Hz to 9.57 Hz with the use of 30 kg/m^3 steel fiber. A similar situation was also presented for the model with 55 cm screw spacing. In this case, the simultaneous use of mesh reinforcement and 30 kg/m^3 steel fiber showed that, the oscillation of the model was increased. In Fig. 15c, the model with the smallest amplitude in the same frequency ranges was the CC55 one. The use of 30kg/m^3 steel fiber with 55 cm screw spacing, was implied the most optimum result.

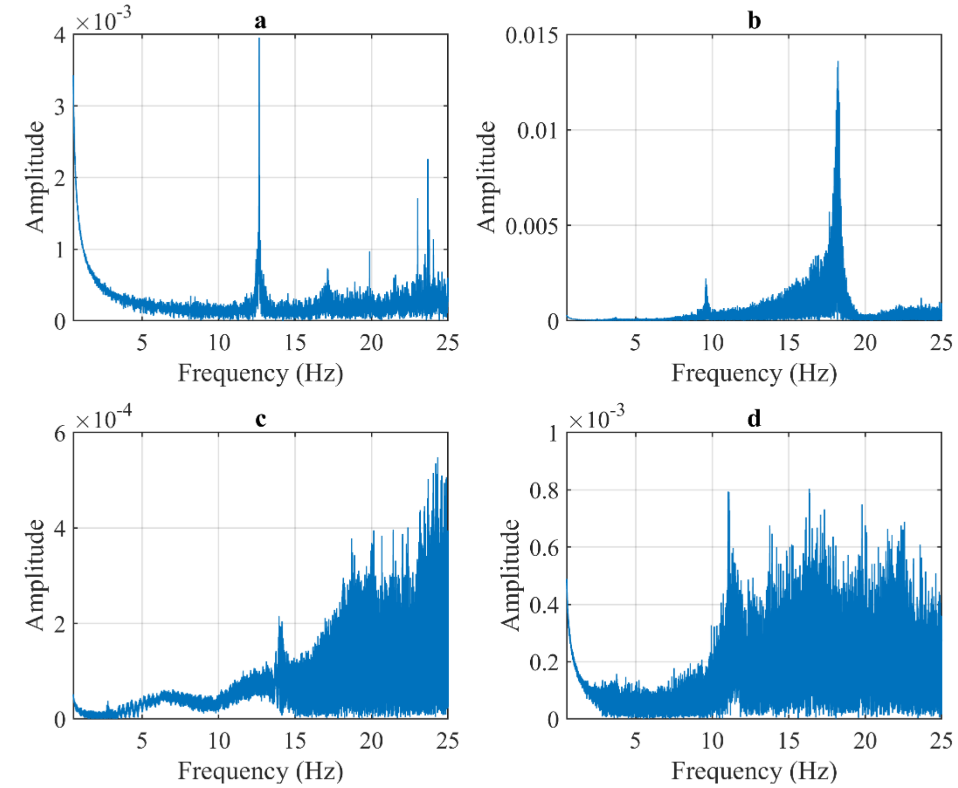

Fig. 15 Frequency of the models containing 30 kg/m^3 steel fiber a) 30SFRC22 b) 30SFRC22M c) 30SFRC55 d) 30SFRC55M

The frequency transforms, obtained for the models with 60 kg/m^3 fibers, were presented in Fig. 16. It was determined that, the dominant frequencies of the 60SFRC22 and 60SFRC22M models were 23.7 and 24.87 Hz, respectively (Fig. 16). As a result of 60 kg/m^3 steel fiber addition to the mix of the models with 22 cm screw spacing and mesh reinforcement; the oscillations were decreased about 18%. The 1st mode frequencies of the 60SFRC55 and 60SFRC55M models were 13.88 and 12.5 Hz (Fig. 16c and Fig. 16d). It was also obtained that 60 kg/m^3 steel fiber addition to the mix was implied a good result by increasing the oscillation of the models with or without mesh, but with 55 cm screw spacing. The oscillations of the models, with 22 cm screw spacing, mesh reinforcement and 60 kg/m^3 steel fiber content, were reduced approximately 56% for 1st group samples. When 30 kg/m^3 steel fiber and mesh reinforcement were used together, the oscillations of the models were increased. However, the addition of 30 kg/m^3 or 60 kg/m^3 steel fiber with 55 cm screw spacing were reduced the oscillations approximately 25% and 24%, respectively. It was predicted that the 60SFRC22M model with 22 cm screw spacing and the 30SFRC55 model with 55 cm screw spacing were the most optimal ones for the oscillations.

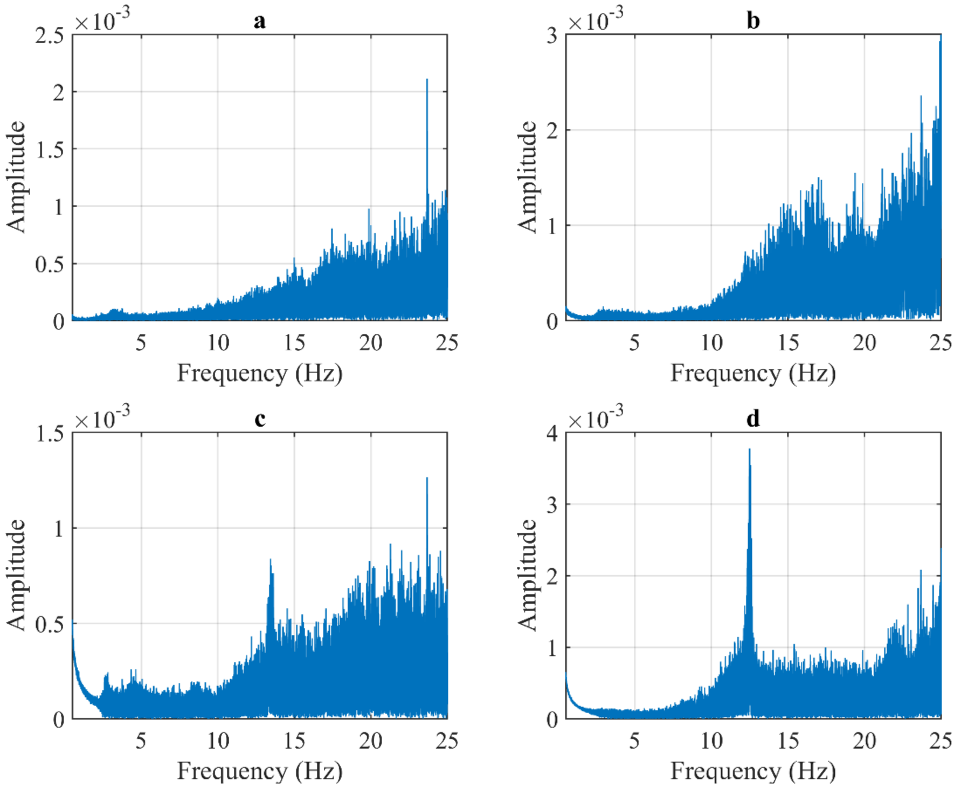

Fig. 16 Frequency of the models with 60 kg/m^3 steel fiber a) 60SFRC22 b) 60SFRC22M c) 60SFRC55 d) 60SFRC55M

The models of 760x720 mm, with 22 cm screw spacing, were inspected after high-temperature process at 600 °C for vibration analysis. Fig. 17 shows the frequency conversions of the models produced by conventional concrete, with and without mesh-reinforcement, before and after high-temperature process at 600 °C. The natural frequencies of the CC22, CC22M, FCC22 and FC22M models were 18.05, 19.07, 14.32, and 13.02 Hz, respectively. The use of mesh reinforcement before the high-temperature process was reduced the oscillations of the model and increased after the high-temperature process. It was determined that keeping the models at 600 °C increased approximately 21% and 32%, respectively, for the models with and without mesh. In addition, the oscillations, with larger amplitude content, were observed for the models after high temperature process (Fig. 17). The use of mesh was increased the oscillations of the model against high-temperature process.

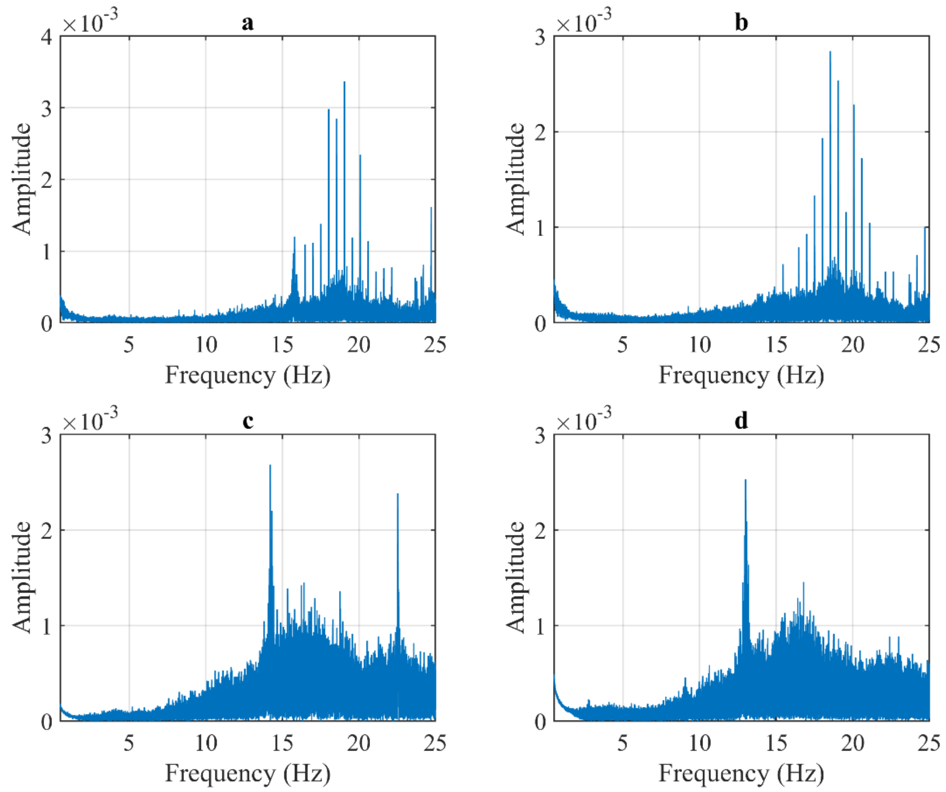

Fig. 17 Frequency of the models without steel fiber exposed to 600 °C temperature process a) CC22 b) C22M c) FCC22 d) FCC22M

The frequency conversions are presented in Fig. 18, after the high-temperature process (600 °C) of the models with 30 kg/m^3 steel fibers. The dominant frequencies of the 30SFRCC22, 30SFRC22M, F30SFRC22, and F30SFRC22M models were determined as 18.49, 13.28, 16.09, and 16.58 Hz, respectively. The emissions were applied by the model increased by 11.2%. The amplitudes of the models were increased about 10% in the dominant frequency ranges after the high-temperature process. The use of mesh was significantly reduced the pre-heat and post-heat amplitudes of the models.

The frequency conversions are presented in Fig. 19, after the high-temperature process (600 °C) of the models with 60 kg/m^3 steel fibers. The dominant natural frequencies of the 60SFRCC22, 60SFRC22M, F60SFRC22, and F60SFRC22M models were determined as 14.32, 13.19, 18.29, and 15.6 Hz, respectively. As a result, it was observed that 30kg/m^3 and 60 kg/m^3 steel fiber content were reduced the emissions of the models, approximately 12% and 22%, respectively. The fact that the model, which was formed by using 60kg/m^3 steel fiber and mesh reinforcement together, especially in the same frequency ranges, produced more amplitude at higher frequencies. Withal, mentioned models were also showed the highest damping capacity [27, 28].

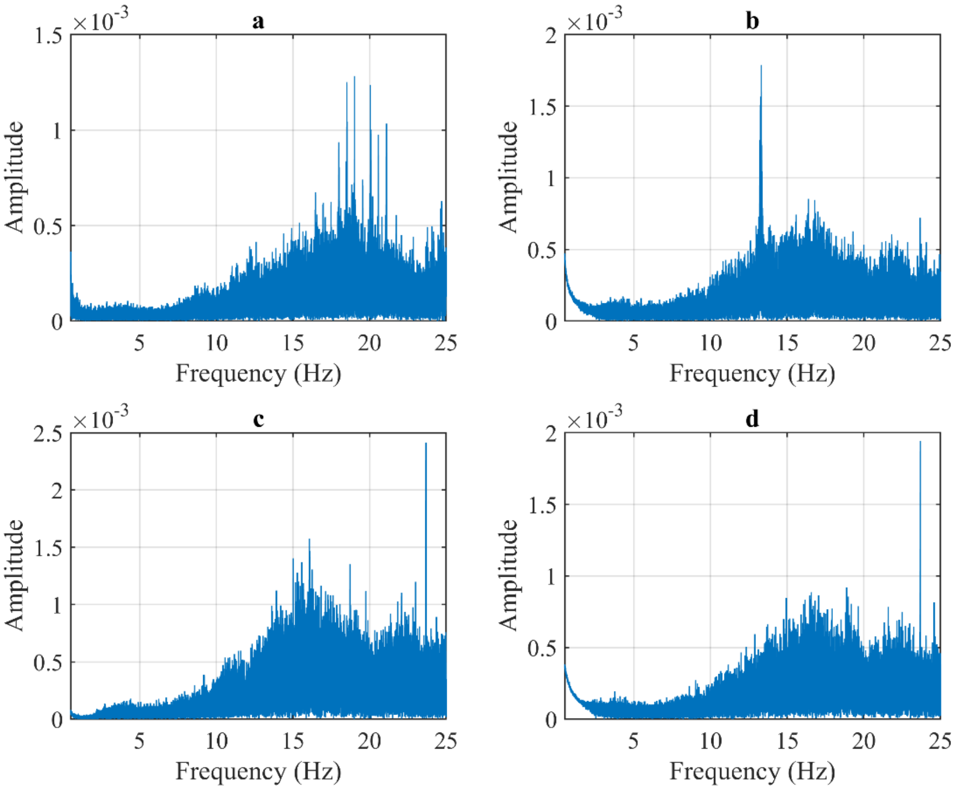

Fig. 18. Frequency of the models with 30 kg/m^3 steel fiber exposed to 600 °C temperature process a) 30SFRCC22 b) 30SFRC22M c) F30SFRC22 d) F30SFRC22M

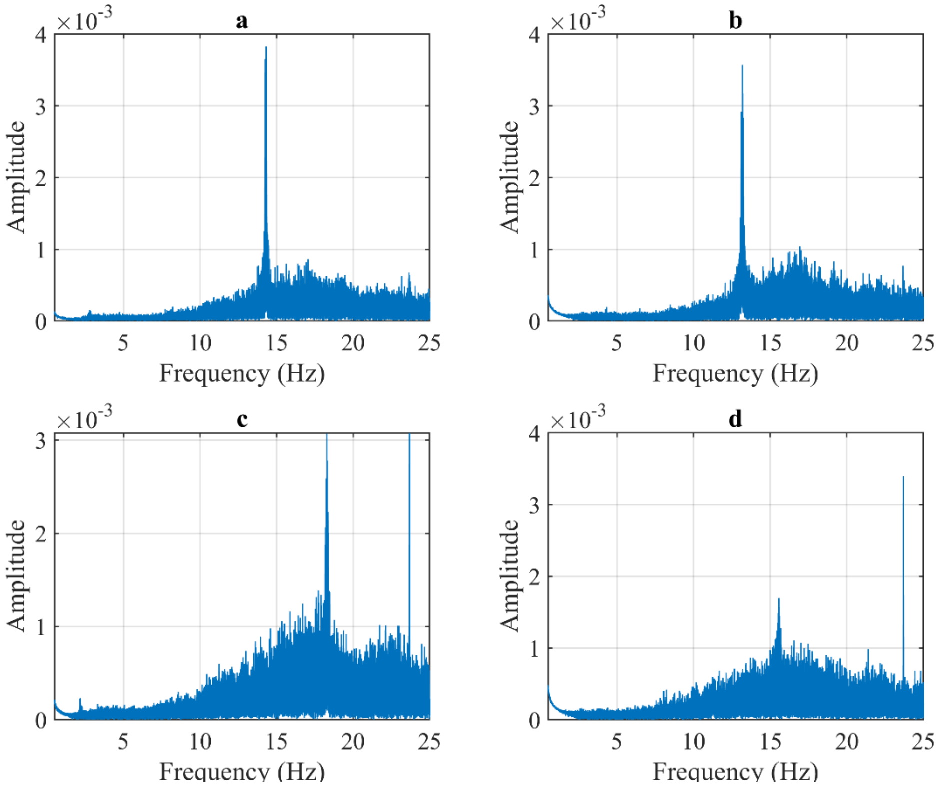

Fig. 19 Frequency of 30 kg/m^3 steel fiber models exposed to 600 °C temperature environment a) 60SFRCC22 b) 60SFRC22M c) F60SFRC22 d) F60SFRC22M

The acceleration response spectral curves have been designed by summing the absolute values of the data in the time history, as a result of vibration tests [29]. The response spectrum gives ideas about the maximum positive accelerations that can occur in the model. Based on the acceleration of the model at the prevailing period values, it has been interpreted to what extent the screw spacing, mesh reinforcements, and steel fibers to reduce the model vibrations.

The response spectrum acceleration graphs were presented in Fig. 20**,** for the 1st group models (1500x1200 mm), without fiber, with 30 kg/m^3, and 60 kg/m^3 fiber content. The maximum acceleration of the CC22, CC22M, CC55 and CC55M models were determined to be 0.0090, 0.0048, 0.018, and 0.0116 m/s^2, respectively. It was determined that reducing the screw spacing from 55 cm to 22 cm, was reduced the acceleration by 50.55%, and the mesh reinforcement was reduced by 46.77% for the same period step. The use of 30 kg/m^3 and 60 kg/m^3 steel fiber in composite flooring increases the reaction acceleration by approximately 44.44% and 18.91%, respectively, in the same screw spacing. In general, the use of 30 kg/m^3 steel fiber and mesh reinforcement in 22 cm and 55 cm screw spacing created high acceleration values, such as, 0.0247 m/s^2 and 0.019 m/s^2, respectively, while also reaches the highest floor vibration acceleration value of 0.056 at 55 cm screw spacing. The steel fiber content of 30 kg/m^3 were produced the highest vibration acceleration values in composite floors (Fig. 20b). The lowest vibration acceleration value in the study was 0.00468 m/s^2 in the case of 60 kg/m^3 steel fiber content and the arrangement of screws at 55 cm spacing without mesh reinforcement (Fig. 20c). Similarly, low acceleration values such as 0.0111 m/s^2 without mesh reinforcement and 0.00689 m/s^2 with mesh reinforcement were produced at 22 cm screw spacing. The test results showed that the composite floor where vibration accelerations were felt the least was 60SFRC55 and the floor where the highest vibration is felt was 30SFRC55.

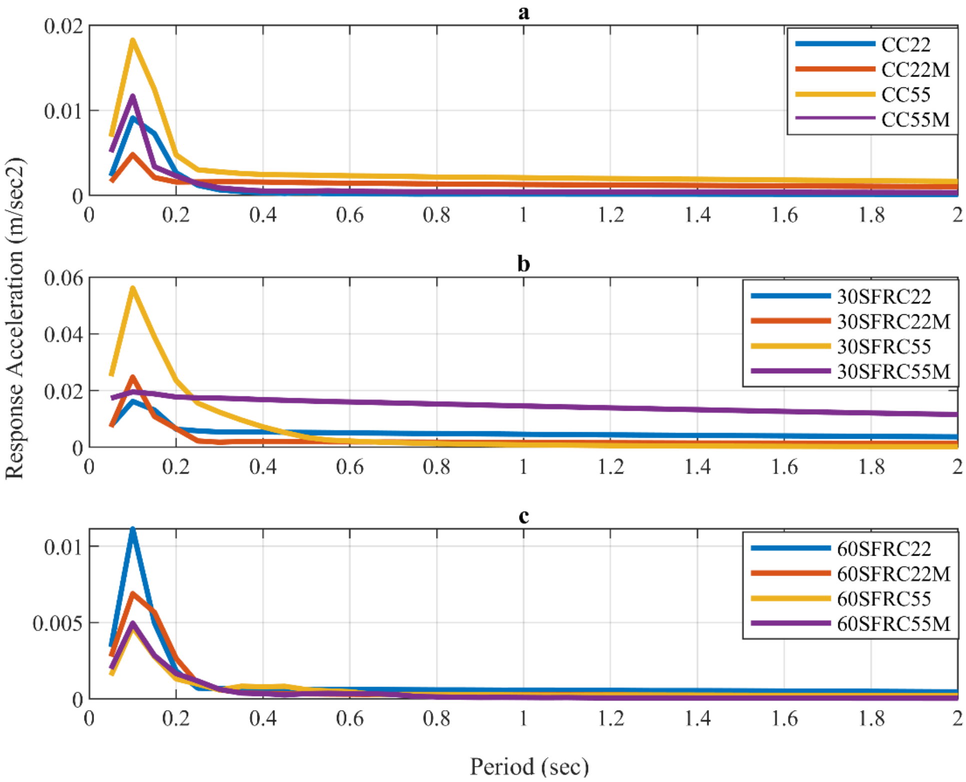

Fig. 20 Response spectra of Group 1 models a) no-fiber models b) Models with 30 kg/m^3 steel fiber c) Models with 60 kg/m^3 steel fiber.

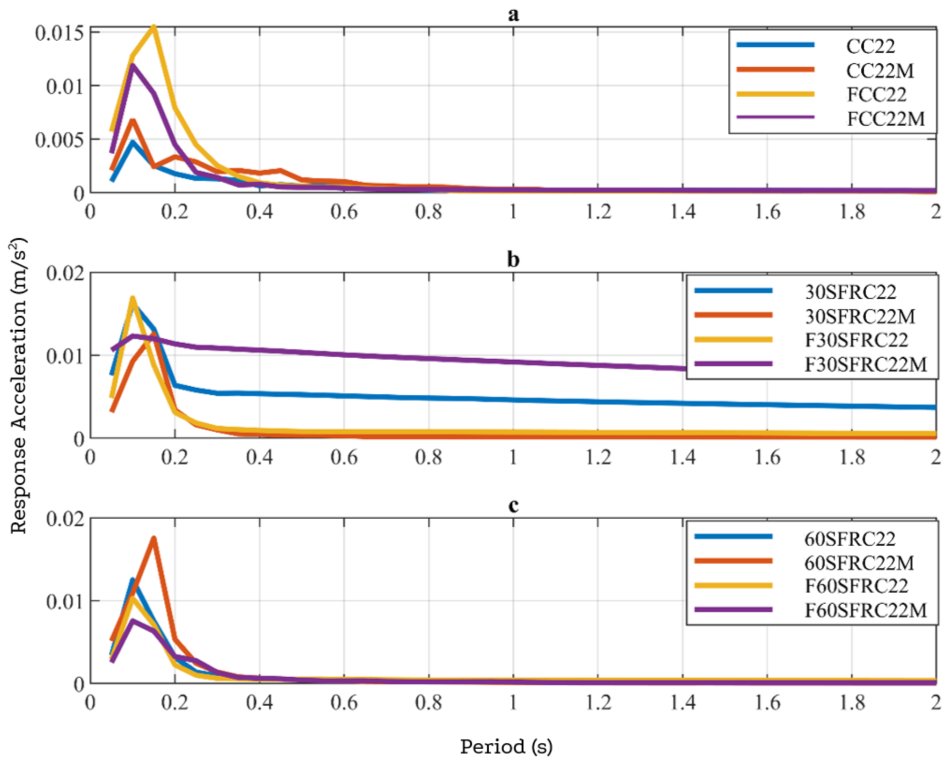

Fig. 21 Response spectra of Group 2 models a) no fiber models b) Models with 30 kg/m^3 steel fiber c) Models with 60 kg/m^3 steel fiber

The response acceleration spectra, for the 760x700 mm, no-fiber, 30 kg/m^3, and 60 kg/m^3 steel fiber models with 22 cm screw spacing and processed for 600℃ (high-temperature condition), were presented in Fig. 21. This result showed that, reducing the size of models also reduces vibrations, as expected. It was observed that the same models reached vibration acceleration values of 0.0115 and 0.0119 m/s^2, respectively. The increase in vibration acceleration after heating process, corresponds to approximately 59% and 42%, respectively. It was observed that the vibration accelerations of the models without or with mesh by using 30 kg/m^3 steel fiber, were increased by 8.28% and 3.25%, respectively. The vibration accelerations of the models, without or with mesh using 60 kg/m^3 steel fiber, were decreased by 33.59% and 36.13%, respectively. Withal, the highest vibration acceleration was observed as 0.0175 m/s^2 for the 60SFRC22M model, and the lowest one was observed for the 30SFRC22 model as 0.0047 m/s^2, among the second group.

The highest vibration acceleration of the F30SFRC22M model was observed as 0.0169 m/s^2, where the lowest one was 0.0047 m/s^2. The vibration acceleration of the model CC22M was determined as 0.0069 m/s^2 before the heating process with the same screw spacing, also. In this case, if the model, with 60 kg/m^3 steel fiber, was exposed to the heating process, the vibration of the model was increased only by 9.21%. However, it was detected that the vibration acceleration of the model, without mesh, was 0.0047 m/s^2 before the heating process. Similarly, the model with 60 kg/m^3 steel fiber, was reached a great value of 0.0103 m/s^2 with an increase of 54%. This result implies that, the 60 kg/m^3 steel fiber content ensures optimum compatibility with the mesh reinforcement and minimizes floor vibrations, also.

4. Conclusion

The vibration response and the bending behavior of 18 model composite floors have been investigated in this study. The effect of bolt spacing, steel-fiber, and mesh reinforcement on the performance of the model composite floors were analyzed, experimentally. Furthermore, the effects of high-temperature on the behavior of the models were examined.

❖ Decreasing the spacings of the screws in the models without mesh reinforcement decreased the peak acceleration response of the steel composite floors. The affectivity of the screw spacing reduction was strikingly decreased by the fiber increase. The effectiveness values were found as 73.2%, 19.5%, and 10.8%, for the models with steel fibers, and 60 kgm^3 steel fibers, respectively.

❖ Using mesh reinforcement was decreased the peak acceleration response of the model composite floors manufactured with conventional concrete. However, using the steel-fiber was increased the peak acceleration response of the models.

❖ When the composite floors were exposed to the high-temperature, the peak acceleration response was increased for the models with conventional concrete, but started to decrease by increasing the amount of the steel fiber content.

❖ Decreasing the bolt spacing and adding the mesh, caused an increase in the energy absorption capacity, maximum load capacity, and maximum displacement of all the models in group 1. Meanwhile, using steel fiber has shown an increase in the energy absorption capacity of the models.

❖ Using the mesh and steel fiber caused an increase in the energy absorption capacity of the high-temperature exposed models (Group 2 models).

❖ Vibration test results show that the model vibrations were reduced by approximately 50% as a result of reducing screw spacing. It has been determined that the model vibrations are reduced by 47% in the case of using mesh reinforcement.

❖ The 60 kg/m^3 steel fiber content can significantly (approximately 54%) reduce possible vibrations that may occur in composite floors when used with mesh reinforcements. In addition, the use of 60 kg/m^3 steel fiber with or without mesh reinforcement in composite floors with screw spacing of 55 cm, the acceleration values were similar to composite floors formed with 22 cm screw spacing.

❖ The use of 60 kg/m^3 steel fiber content together with the mesh reinforcement is effective in reducing the vibrations of composite floors after the high-temperature process. The vibrations of the composite model floors prepared before the heat process and formed with conventional concrete at 22 cm screw spacing, increased by approximately 9% compared to the vibrations of the other models when exposed to high-temperature process with the addition of 60 kg/m^3 steel fiber and mesh reinforcement, and became the most recommended flooring type.

❖ The deformation, energy absorption capacities, floor vibrations, and the fire resistance are considered; the applicable flooring type is 60SFRC22M composite flooring with 60kg/m^3 steel fiber, 22 cm screw spacing, mesh reinforcement and traditional concrete.

❖ The results showed that the amount of steel fiber should be optimally adjusted for the mesh reinforcement and steel fiber to work in harmony. It is also foreseen that if a high amount of steel fiber content is used, the screw spacing should be adjusted according to this ratio.

Acknowledgment

The research is part of the Sadiq Ahmad Afzali master thesis and Ataturk University Projects FYL-2019-7293. The author would like to thank Ataturk University for funding the projects.

Declaration of competing interest

The authors declare that they have no known competing financial interests or personal relationship that could have appeared to influence the work reported in this paper.

References

[1] A. Chatteree, S. Chandra, Thin-slab casting: new possibilities, Sadhana 26 (2001) 163-178
[2] J. Qureshi, D. Lam, J. Ye, The influence of profiled sheeting thickness and shear connector's position on strength and ductility of headed shear connector, Engineering Structures 33(5) (2011) 1643-1656.https://doi.org/10.1016/j.engstruct.2011.01.035
[3] S. Gopinath, A. Prakash, R. Aahrthy, M.B. Harish, Investigations on the influence of matrix and textile on the response of textile reinforced concrete slabs under impact loading, Sādhan ā 43 (2018) 1-11.https://doi.org/10.1007/s12046-018-0933-8
[4] S. Nayar, R. Gettu, Mechanistic-empirical design of fibre reinforced concrete (FRC) paveme nts using inelastic analysis, Sādhanā 45(1) (2020) 19.https://doi.org/10.1007/s12046-019-12 55-1
[5] P.M. Choradiya, P.D. Kumbhar, Behaviour of concrete deck slab using shear connectors: A review, International Journal of Innovative Research in Science, Engineering Technology 4 (12) (2015) 12883-12892
[6] H. Wright, H. Evans, P. Harding, The use of profiled steel sheeting in floor construction, Jou rnal of Constructional Steel Research 7(4) (1987) 279-295
[7] J.W. Luo, Behaviour and analysis of steel fibre-reinforced concrete under reversed cyclic loa ding, University of Toronto (Canada)2014.
[8] W.D. Varela, R.C. Battista, Control of vibrations induced by people walking on large span c omposite floor decks, Engineering Structures 33(9) (2011) 2485-2494.https://doi.org/10.101 6/j.engstruct.2011.04.021
[9] A. Pavic, M. Willford, Vibration Serviceability of Posttensioned Concrete Floors. Post-Tens ioned Concrete Floors Design Handbook, Appendix G, Technical Report 43, 2005.
[10] A. Ferreira, G. Fasshauer, Analysis of natural frequencies of composite plates by an RBF-ps eudospectral method, Composite Structures 79(2) (2007) 202-210.https://doi.org/10.1016/j.c ompstruct.2005.12.004
[11] Y.K. Ju, D.-Y. Kim, S.-D. Kim, S.-W. Yoon, Y.-K. Lee, D.-H. Kim, Dynamic characteristic s of the new composite floor system, Steel Structures 8 (2008) 347-356
[12] F.A. Gandomkar, W.H.W. Badaruzzaman, S.A. Osman, The natural frequencies of composit e Profiled Steel Sheet Dry Board with Concrete infill (PSSDBC) system, Latin American Jo urnal of Solids Structures 8 (2011) 351-372
[13] F. Gandomkar, W. Wan Badaruzzaman, S. Osman, A. Ismail, Experimental and numerical i nvestigation of the natural frequencies of the composite profiled steel sheet dry board (PSSD B) system, Journal of the South African Institution of Civil Engineering= Joernaal van die S uid-Afrikaanse Instituut van Siviele Ingenieurswese 55(1) (2013) 11-21
[14] H. Cifuentes, F. Medina, Experimental study on shear bond behavior of composite slabs acc ording to Eurocode 4, Journal of Constructional Steel Research 82 (2013) 99-110.https://doi. org/10.1016/j.jcsr.2012.12.009
[15] S.J. Hicks, A.L. Smith, Stud shear connectors in composite beams that support slabs with pr ofiled steel sheeting, Structural Engineering International 24(2) (2014) 246-253.https://doi.o rg/10.2749/101686614X13830790993122
[16] L. Costa-Neves, J.S. da Silva, L. De Lima, S. Jordão, Multi-storey, multi-bay buildings with composite steel-deck floors under human-induced loads: The human comfort issue, Comput ers Structures 136 (2014) 34-46.https://doi.org/10.1016/j.compstruc.2014.01.027
[17] K. Jarnerö, A. Brandt, A. Olsson, Vibration properties of a timber floor assessed in laborator y and during construction, Engineering Structures 82 (2015) 44-54.https://doi.org/10.1016/j. engstruct.2014.10.019
[18] J. Holomek, M. Bajer, M. Vild, Cast screws as shear anchors for composite slabs, Procedia E ngineering 195 (2017) 114-119
[19] TS802, Turkish Standard -Design of concrete mixes, Ankara, Turkey, (2016)
[20] TS/EN-14889-1, Fibres for concrete - Part 1: Steel fibres - Definitions, specifications and co nformity, Ankara, Turkey, (2016)
[21] TS4559, Steel Mesh for Concrete, Ankara, Turkey, (2006)
[22] TS/EN/12390-3, Compressive strength of test specimens, (2019)
[23] TS/EN/12390-5, Flexural strength of test specimens, (2019)
[24] Eurocode-4, Design of composite steel concrete structures, Part 1.1: General rules and rules for buildings, European Committee for Standardization (CEN), (2004)
[25] P. Wessel, W.H. Smith, R. Scharroo, J. Luis, F. Wobbe, Generic mapping tools: improved v ersion released, Transactions American Geophysical Union 94(45) (2013) 409-410
[26] A. Chopra, Dynamics of Structures: Theory and Applications to Earthquake Engineering, Pr entice Hall, Englewood Cliffs, NJ 1995.
[27] K. Beyen, Damage identification analyses of a historic masonry structure in TF domain, Jour nal of Technical 32(2) (2021) 10577-10610
[28] O. Sak, K. Beyen, Damage analysis of the structures in time-frequency domain with wavelet transform method, Journal of Technical 30 (2019)
[29] S. Rajasekaran, Structural dynamics of earthquake engineering: theory and application using MATHEMATICA and MATLAB, Elsevier2009.